nature

https://doi.org/10.1038/s41586-021-03777-9

Accelerated Article Preview

Reduced sensitivity of SARS-CoV-2 variant Delta to antibody neutralization

Received: 26 May 2021

Accepted: 29 June 2021

Accelerated Article Preview Published online 8 July 2021

Cite this article as: Planas, D. et al. Reduced sensitivity of SARS-CoV-2 variant Delta to antibody neutralization. *Nature* https://doi.org/10.1038/s41586-021-03777-9 (2021).

Delphine Planas, David Veyer, Artem Baidaliuk, Isabelle Staropoli, Florence Guivel-Benhassine, Maaran Michael Rajah, Cyril Planchais, Françoise Porrot, Nicolas Robillard, Julien Puech, Matthieu Prot, Floriane Gallais, Pierre Gantner, Aurélie Velay, Julien Le Guen, Najibi Kassis-Chikhani, Dhiaeddine Edriss, Laurent Belec, Aymeric Seve, Laura Courtellemont, Hélène Péré, Laurent Hocqueloux, Samira Fafi-Kremer, Thierry Prazuck, Hugo Mouquet, Timothée Bruel, Etienne Simon-Lorière, Felix A. Rey & Olivier Schwartz

Article

Reduced sensitivity of SARS-CoV-2 variant Delta to antibody neutralization

https://doi.org/10.1038/s41586-021-03777-9

Received: 26 May 2021

Accepted: 29 June 2021

Published online: 8 July 2021

Delphine Planas[1,2], David Veyer[3,4], Artem Baidaliuk[5], Isabelle Staropoli[1], Florence Guivel-Benhassine[1], Maaran Michael Rajah[1,6], Cyril Planchais[7], Françoise Porrot[1], Nicolas Robillard[4], Julien Puech[4], Matthieu Prot[5], Floriane Gallais[8,9], Pierre Gantner[8,9], Aurélie Velay[8,9], Julien Le Guen[10], Najibi Kassis-Chikhani[11], Dhiaeddine Edriss[4], Laurent Belec[4], Aymeric Seve[12], Laura Courtellemont[12], Hélène Péré[3], Laurent Hocqueloux[12], Samira Fafi-Kremer[8,9], Thierry Prazuck[12], Hugo Mouquet[7], Timothée Bruel[1,2,14]✉, Etienne Simon-Lorière[5,14], Felix A. Rey[13,14] & Olivier Schwartz[1,2,14]✉

The SARS-CoV-2 B.1.617 lineage was identified in October 2020 in India[1–5]. It has since then become dominant in some indian regions and UK and further spread to many countries[6]. The lineage includes three main subtypes (B1.617.1, B.1.617.2 and B.1.617.3), harbouring diverse Spike mutations in the N-terminal domain (NTD) and the receptor binding domain (RBD) which may increase their immune evasion potential. B.1.617.2, also termed variant Delta, is believed to spread faster than other variants. Here, we isolated an infectious Delta strain from a traveller returning from India. We examined its sensitivity to monoclonal antibodies (mAbs) and to antibodies present in sera from COVID-19 convalescent individuals or vaccine recipients, in comparison to other viral strains. Variant Delta was resistant to neutralization by some anti-NTD and anti-RBD mAbs including Bamlanivimab, which were impaired in binding to the Spike. Sera from convalescent patients collected up to 12 months post symptoms were 4 fold less potent against variant Delta, relative to variant Alpha (B.1.1.7). Sera from individuals having received one dose of Pfizer or AstraZeneca vaccines barely inhibited variant Delta. Administration of two doses generated a neutralizing response in 95% of individuals, with titers 3 to 5 fold lower against Delta than Alpha. Thus, variant Delta spread is associated with an escape to antibodies targeting non-RBD and RBD Spike epitopes.

The variant Delta has been detected in many countries. It has become predominant in the state of Maharashtra and probably other Indian regions[4] and represented 77% of sequenced viruses circulating in UK between June 2 and 9, 2021[6]. It has been classified as a Variant of Concern (VOC) and is believed to be 60% more transmissible than variant Alpha. Little is known about its sensitivity to the humoral immune response. Recent reports indicated a reduced sensitivity of members of the B.1.617 lineage to certain monoclonal and polyclonal antibodies[1–5,7–9].

Isolation and characterization of the variant Delta

We isolated the variant Delta from a nasopharyngeal swab of a symptomatic individual, a few days upon his return to France from India. The virus was amplified by two passages on Vero E6 cells. Sequences of the swab and the outgrown virus were identical and identified the variant Delta (GISAID accession ID: EPI_ISL_2029113) (Extended Data Fig. 1). In particular, the Spike protein contained 9 mutations, when compared to the D614G strain (belonging to the basal B.1 lineage) used here as a reference, including five mutations in the NTD (T19R, G142D, Δ156, Δ157, R158G), two in the RBD (L452R, T478K), one mutation close to the furin cleavage site (P681R) and one in the S2 region (D950N) (Extended Data Fig. 1). This set of mutation was different from those observed in other members of the B.1.617 lineage and other VOCs (Extended Data Fig. 1). Viral stocks were titrated using S-Fuse reporter cells and Vero cells[10,11]. Viral titers were similar in the two target cells and reached 10^5-10^6 infectious units/ml. Large syncytia expressing the Spike were observed in Delta-infected cells (Extended Data Fig. 2). Future work will help determining whether Delta is more fusogenic than other variants, as suggested here by the large size of Delta-induced syncytia.

[1]Virus & Immunity Unit, Department of Virology, Institut Pasteur, CNRS UMR 3569, Paris, France. [2]Vaccine Research Institute, Creteil, France. [3]INSERM, Functional Genomics of Solid Tumors (FunGeST), Centre de Recherche des Cordeliers, Université de Paris and Sorbonne Université, Paris, France. [4]Hôpital Européen Georges Pompidou, Laboratoire de Virologie, Service de Microbiologie, Paris, France. [5]G5 Evolutionary genomics of RNA viruses, Department of Virology, Institut Pasteur, Paris, France. [6]Université de Paris, Sorbonne Paris Cité, Paris, France. [7]Laboratory of Humoral Immunology, Department of Immunology, Institut Pasteur, INSERM U1222, Paris, France. [8]CHU de Strasbourg, Laboratoire de Virologie, Strasbourg, France. [9]Université de Strasbourg, INSERM, IRM UMR_S 1109, Strasbourg, France. [10]Hôpital Européen Georges Pompidou, Service de Gériatrie, Assistance Publique des Hôpitaux de Paris, Paris, France. [11]Hôpital européen Georges Pompidou, Unité d'Hygiène Hospitalière, Service de Microbiologie, Assistance Publique-Hôpitaux de Paris, Paris, 75015, France. [12]CHR d'Orléans, service de maladies infectieuses, Orléans, France. [13]Structural Virology Unit, Department of Virology, Institut Pasteur, CNRS UMR 3569, Paris, France. [14]These authors contributed equally: Timothée Bruel, Etienne Simon-Lorière, Felix A. Rey, Olivier Schwartz. ✉e-mail: timothee.bruel@pasteur.fr; olivier.schwartz@pasteur.fr

Phylogenetic analysis of the B.1.617 lineage

To contextualize the Delta isolate reported here, we inferred a global phylogeny subsampling the diversity of SARS-CoV-2 sequences available on the GISAID EpiCoV database (Extended Data Fig. 3). The B.1.617 lineage, subdivided into three sublineages according to the PANGO classification[12], derives from the B.1 lineage (D614G). The three sublineages present multiple changes in the Spike, including the L452R substitution in the RBD, already seen in other variants such as B.1.429 and P681R, located in the furin cleavage site and which may enhance Spike fusogenic activity[13]. The E484Q substitution, which may be functionally similar to the antibody-escape mutation E484K found in variants Beta and Gamma (B.1.351 and P.1), is present in B.1.617.1 and B.1.617.3, and has likely reverted in the Delta sublineage, as it was present in a sequence (B.1.617) ancestral to the three sublineages (Extended Data Fig. 1)[14]. Whether the absence of E484Q, the presence of T478K, other changes in the Spike or elsewhere may facilitate viral replication and transmissibility remains unknown. Interestingly, the B.1.617 lineage is not homogeneous, with multiple mutations fixed in a sublineage (e.g. Spike:T19R, G142D or D950N) also detected at lower frequencies in other sublineages. This may reflect founder effects or similar selective pressures acting on these emerging variants.

Mutational changes in variant Delta

The locations of the Spike mutations in the variant Delta showed a similar overall distribution to those that appeared in other VOCs. In particular, in addition to D614G, the D950N mutation mapped to the trimer interface (Extended Data Fig. 4a), suggesting a potential contribution in regulating Spike dynamics, as shown with D614G[13]. As with other VOCs, some mutations in Delta cluster in the NTD (Extended Data Fig. 4b). The 156-157 deletion and G158R mutation map to the same surface as the 144 and 241-243 deletions in variants Alpha and Beta (B.1.351), respectively. The T19R maps to the surface patch that has several mutations in Alpha. These altered residues lie in the NTD "supersite" targeted by most anti-NTD neutralizing antibodies[15]. In the RBD, mutations appearing in VOCs map to the periphery of the ACE2 binding surface (Extended Data Fig. 4c), suggesting that the virus accumulates mutations there to reduce or avoid antibody recognition while maintaining binding to ACE2. For instance, the L452R mutation found in Delta impairs neutralization by antibodies[16] and is located at this periphery. The only mutation within the ACE2 patch is at location 501, which increases affinity of the RBD for ACE2 and is also involved in antibody escape[13]. The T478K mutation in the RBD is unique to Delta and falls within the epitope region of potent neutralizing mAbs categorized as "Class 1" (Extended Data Fig. 4c)[17]. This mutation is close to the E484K mutation that facilitates antibody escape[13]. These observations prompted us to analyze the neutralization potential of mAbs and sera from convalescents and vaccinees against variant Delta.

Neutralization of variant Delta by monoclonal antibodies

We assessed the sensitivity of Delta to a panel of human mAbs using the S-Fuse assay. We tested four clinically approved mAbs, Bamlanivimab (LY-CoV555), Etesevimab (LY-CoV016), Casirivimab (REGN10933) and Imdevimab (REGN10987) targeting the RBD[18,19] as well as eight anti-RBD (RBD-48, RBD-85, RBD-98 and RBD-109) and anti-NTD (NTD-18, NTD-20, NTD-69 and NTD-71) mAbs derived from convalescent individuals (Planchais et al, in preparation). Neutralizing anti-RBD mAbs can be classified into 4 main categories[17,20]. RBD-48 and RBD-85 belong to the first category ("Class 1") and act by blocking binding of the "up" conformation of RBD to ACE2[17]. The precise epitopes of RBD-98 and RBD-109 are not yet defined but overlap with those of RBD-48 and RBD-85. The anti-NTD antibodies bind uncharacterized epitopes.

We measured the potency of the four therapeutic antibodies against variant Delta and included as a comparison D614G (B.1), Alpha and Beta variants. The antibodies neutralized D614G, with IC50 (Inhibitory Concentration 50%) varying from 1.2×10^{-3} to 6.5×10^{-2} µg/mL (Fig. 1). Etesivimab displayed a 200-fold increase of IC50 against Alpha. As previously reported, Bamlanivimab and Etesivimab did not neutralize Beta[21]. Bamlanivimab lost antiviral activity against Delta, in line with previous results demonstrating that L452R is an escape mutation for this mAb[16]. Etesivimab, Casirivimab and Imdevimab remained active against Delta (Fig. 1).

The four other anti-RBD mAbs neutralized D614G. The IC50 of RBD-48 and RBD-98 were about 15-100-fold higher with Alpha than with D614G, whereas RBD-85 displayed increased activity against Alpha. Three mAbs inhibited Delta whereas RBD-85 was inactive (Extended Data Fig. 5).

The four anti-NTD mAbs were globally less efficient than anti-RBD mAbs. They inhibited D614G with high IC50 (1-60 µg/mL) (Extended Data Fig. 5). Three anti-NTD antibodies lost activity against Alpha and Delta, whereas the fourth (NTD-18) inhibited to some extent the two variants. Thus, Delta escapes neutralization by some antibodies targeting the RBD or NTD.

We examined by flow cytometry the binding of each mAb to Vero cells infected with the different variants. Radar plots show the binding of all antibodies tested (Extended Data Fig. 6). D614G was recognized by the 12 mAbs tested. Alpha and Delta were recognized by 9 and 7 mAb, respectively. Bamlanivimab no longer bound Delta. We also analyzed the binding of the 12 mAbs to variant Beta, which is more resistant to neutralization. Bamlanivimab and Etesivimab lost their binding to Beta and only 5 of the antibodies bound this variant (Extended Data Fig. 6). Thus, escape of Delta and other variants to neutralization is due to a reduction or loss of binding of the antibodies.

Sensitivity of variant Delta to sera from convalescent individuals

We examined the neutralization ability of sera from convalescent subjects. We first selected samples from 56 donors in a cohort of infected individuals from the French city of Orléans. All individuals were diagnosed with SARS-CoV-2 infection by RT-qPCR or serology and included critical, severe, mild-to-moderate and asymptomatic cases (Extended Data Table 1). They were not vaccinated at the sampling time. We recently characterized the potency of these sera against D614G, Alpha and Beta isolates[11]. We analyzed individuals sampled at a median of 188 days post onset of symptoms (POS), referred to as Month 6 (M6) samples. We calculated ED50 (Effective Dose 50%) for each combination of serum and virus (Extended Data Fig. 7a). With the Alpha variant, we obtained similar ED50 values in this series of experiments than in our previous analysis[11] (Extended Data Fig. 7b). We thus included our published data for D614G and Beta in the comparison. With Delta, neutralization titers were significantly decreased by 4 to 6-fold when compared to Alpha and D614G strains, respectively (Extended Data Fig. 7a). This reduction in neutralizing titers was similar against Delta and Beta (Extended Data Fig. 7a).

We asked whether this neutralization profile was maintained for longer periods of time. We analyzed sera from 47 individuals from another cohort of RT-qPCR-confirmed health care workers from Strasbourg University Hospitals who experienced mild disease[22,23]. Twenty six individuals were unvaccinated, whereas 21 received a single dose of vaccine 7-81 days before sampling. The samples were collected at a later time point (M12), with a median of 330 and 359 days for unvaccinated and vaccinated individuals, respectively (Extended Data Table 1)[23]. As observed[23], the neutralization activity was globally low at M12 in unvaccinated individuals (Fig. 2a). There was a 4 fold decrease of ED50 against Beta and Delta, relative to Alpha (Fig. 2a). The 21 single-dose vaccine recipients of the M12 cohort included 9 vaccinated with AstraZeneca, 9 with Pfizer and 3 with Moderna vaccines. Sera from these vaccinated participants showed a dramatic increase in neutralizing antibody titers

against Alpha, Beta and Delta variants, as compared to unvaccinated convalescents (Fig. 2a). Therefore, as shown with other variants[23,24], a single dose of vaccine boosts cross-neutralizing antibody responses to Delta.

We then classified the cases as neutralizers (defined as harboring neutralizing antibodies detectable at the first serum dilution of 1/30) and non-neutralizers, for the viral variants and the two cohorts (Extended Data Fig. 7c). Between 76% and 92% of the individuals neutralized the four strains at M6. The fraction of neutralizers was lower in the second cohort at M12, a phenomenon which was particularly marked for Beta and Delta. 88% of individuals neutralized Alpha and only 47% neutralized Delta. After vaccination, 100% of convalescent individuals neutralized the four strains (Extended Data Fig. 7c).

Thus, variant Delta displays enhanced resistance to neutralization by sera from unvaccinated convalescent individuals, particularly one year after infection.

Sensitivity of variant Delta to sera from vaccine recipients

We next asked whether vaccine-elicited antibodies neutralized variant Delta in individuals that were not previously infected with SARS-CoV-2. We randomly selected 59 individuals from a cohort of vaccinated subjects established in Orléans. The characteristics of vaccinees are depicted in Extended Data Table 2. 16 individuals received the Pfizer vaccine. They were sampled at week 3 (W3) after the first dose and W8 (corresponding to week 5 after the second dose). 13 individuals were also sampled at W16. 43 individuals received the AstraZeneca vaccine. Sera from 23 individuals were sampled after one dose (W10) and from 20 other individuals after two doses (W16, corresponding to week 4 after the second dose). We measured the potency of the sera against D614G, Alpha, Beta and Delta strains (Fig. 2b,c).

With the Pfizer vaccine, after a single dose (W3), the levels of neutralizing antibodies were low against D614G, and almost undetectable against Alpha, Beta and Delta variants (Fig. 2b). Titers significantly increased after the second dose. We observed a 3-fold and 16-fold reduction in the neutralization titers against Delta and Beta, respectively, when compared to Alpha (Fig. 2b). Similar differences between strains were observed at a later time point (W16), although titers were globally slightly lower (Extended Data Fig. 7b).

A similar pattern was observed with the AstraZeneca vaccine. It induced low levels of antibodies neutralizing Delta and Beta, when compared to D614G and Alpha, after a single dose (W10) (Fig. 2c). Four weeks after the second dose (W16), neutralizing titers were strongly increased. There was however a 5-fold and 9-fold reduction in neutralization titers against Delta and Beta, respectively, relative to Alpha (Fig. 2c).

We classified the vaccine recipients as neutralizers and non-neutralizers, for the four viral strains (Extended Data Fig. 7d,e). With Pfizer, 13% of individuals neutralized the variant Delta after a single dose. 81 to 100% of individuals neutralized any of the four stains after the second dose, at W8. This fraction remained stable at W16, with the exception of variant Beta, which was neutralized by only 46% of the individuals. 74% and 61% of individuals that received a single dose of AstraZeneca vaccine neutralized D614G and Alpha strains, respectively. This fraction sharply dropped with Beta and Delta variants, which were inhibited by only 4 and 9% of the sera. Four weeks after the second dose of AstraZeneca, 95-100% of individuals neutralized the four strains.

Therefore, a single dose of Pfizer or AstraZeneca was either poorly or not at all efficient against Beta and Delta variants. Both vaccines generated a neutralizing response that efficiently targeted variant Delta only after the second dose.

Discussion

We studied the cross-reactivity of mAbs to pre-existing SARS-CoV-2 strains, sera from long-term convalescent individuals and recent vaccine recipients against an infectious Delta isolate. Some mAbs, including Bamlavinimab, lost binding to the Spike and no longer neutralized variant Delta. We further show that Delta is less sensitive to sera from naturally immunized individuals. Vaccination of convalescent individuals boosted the humoral immune response well above the threshold of neutralization. These results strongly suggest that vaccination of previously infected individuals will be most likely protective against a large array of circulating viral strains, including variant Delta.

In individuals that were not previously infected with SARS-CoV-2, a single dose of either Pfizer or AstraZeneca vaccines barely induced neutralizing antibodies against variant Delta. About 10% of the sera neutralized this variant. However, a two-dose regimen generated high sero-neutralization levels against variants Alpha, Beta and Delta, in subjects sampled at W8 to W16 post vaccination. Neutralizing antibody levels are highly predictive of immune protection from symptomatic SARS-CoV-2 infection[25]. A recent report analyzing all sequenced symptomatic cases of COVID-19 in England was used to estimate the impact of vaccination on infection[26]. Effectiveness was notably lower with Delta than with Alpha after one dose of AstraZeneca or Pfizer vaccines. The two-dose effectiveness against Delta was estimated to be 60% and 88% for AstraZeneca and Pfizer vaccines, respectively[26]. Our neutralization experiments indicate that Pfizer and AstraZeneca vaccine-elicited antibodies are efficacious against variant Delta, but about 3-5 fold less potent than against variant Alpha. There was no major difference in the levels of antibodies elicited by Pfizer or AstraZeneca vaccines.

Potential limitations of our work include a low number of vaccine recipients analyzed and the lack of characterization of cellular immunity, which may be more cross-reactive than the humoral response. Future work with more individuals and longer survey periods will help characterize the role of humoral responses in vaccine efficacy against circulating variants.

Our results demonstrate that the emerging variant Delta partially but significantly escapes neutralizing mAbs, and polyclonal antibodies elicited by previous SARS-CoV-2 infection or vaccination.

Online content

Any methods, additional references, Nature Research reporting summaries, source data, extended data, supplementary information, acknowledgements, peer review information; details of author contributions and competing interests; and statements of data and code availability are available at https://doi.org/10.1038/s41586-021-03777-9.

1. Yadav, P. D. *et al*. Neutralization of variant under investigation B.1.617 with sera of BBV152 vaccinees. *Clinical Infectious Diseases*, https://doi.org/10.1093/cid/ciab411 (2021).
2. Ferreira, I. *et al*. SARS-CoV-2 B.1.617 emergence and sensitivity to vaccine-elicited antibodies. *Biorxiv*, 2021.2005.2008.443253, https://doi.org/10.1101/2021.05.08.443253 (2021).
3. Hoffmann, M. *et al*. SARS-CoV-2 variant B.1.617 is resistant to Bamlanivimab and evades antibodies induced by infection and vaccination. *Biorxiv*, 2021.2005.2004.442663, https://doi.org/10.1101/2021.05.04.442663 (2021).
4. Cherian, S. *et al*. Convergent evolution of SARS-CoV-2 spike mutations, L452R, E484Q and P681R, in the second wave of COVID-19 in Maharashtra, India. *Biorxiv*, 2021.2004.2022.440932, https://doi.org/10.1101/2021.04.22.440932 (2021).
5. Edara, V.-V. *et al*. Infection and vaccine-induced neutralizing antibody responses to the SARS-CoV-2 B.1.617.1 variant. *Biorxiv*, 2021.2005.2009.443299, https://doi.org/10.1101/2021.05.09.443299 (2021).
6. Public Health England. Variants distribution of cases. *https://www.gov.uk/government/publications/covid-19-variants-genomically-confirmed-case-numbers/variants-distribution-of-case-data-11-june-2021* (2021).
7. Tada, T. *et al*. The Spike Proteins of SARS-CoV-2 B.1.617 and B.1.618 Variants Identified in India Provide Partial Resistance to Vaccine-elicited and Therapeutic Monoclonal Antibodies. *Biorxiv*, 2021.2005.2014.444076, https://doi.org/10.1101/2021.05.14.444076 (2021).
8. Liu, J. *et al*. BNT162b2-elicited neutralization of B.1.617 and other SARS-CoV-2 variants. *Nature*, https://doi.org/10.1038/s41586-021-03693-y (2021).
9. Wall, E. C. *et al*. Neutralising antibody activity against SARS-CoV-2 VOCs B.1.617.2 and B.1.351 by BNT162b2 vaccination. *The Lancet* **397**, 2331-2333, https://doi.org/10.1016/S0140-6736(21)01290-3 (2021).
10. Buchrieser, J. *et al*. Syncytia formation by SARS-CoV-2 infected cells. *The EMBO Journal*, e106267, https://doi.org/10.15252/embj.2020106267 (2020).
11. Planas, D. *et al*. Sensitivity of infectious SARS-CoV-2 B.1.1.7 and B.1.351 variants to neutralizing antibodies. *Nature Medicine* **27**, 917-924, (2021).

12. Rambaut, A. *et al*. A dynamic nomenclature proposal for SARS-CoV-2 lineages to assist genomic epidemiology. *Nature Microbiology* **5**, 1403-1407, (2020).
13. Plante, J. A. *et al*. The variant gambit: COVID-19's next move. *Cell Host & Microbe* **29**, 508-515, (2021).
14. CDC. SARS-CoV-2 Variant Classifications and Definitions. https://www.cdc.gov/coronavirus/2019-ncov/cases-updates/variant-surveillance/variant-info.html (2021).
15. McCallum, M. *et al*. N-terminal domain antigenic mapping reveals a site of vulnerability for SARS-CoV-2. *Cell* **184**, 2332-2347.e2316, (2021).
16. Starr, T. N., Greaney, A. J., Dingens, A. S. & Bloom, J. D. Complete map of SARS-CoV-2 RBD mutations that escape the monoclonal antibody LY-CoV555 and its cocktail with LY-CoV016. *Cell Reports Medicine* **2**, 100255, (2021).
17. Barnes, C. O. *et al*. SARS-CoV-2 neutralizing antibody structures inform therapeutic strategies. *Nature* **588**, 682-687, PMID - 33045718 (2020).
18. Taylor, P. C. *et al*. Neutralizing monoclonal antibodies for treatment of COVID-19. *Nature Reviews Immunology* **21**, 382-393, (2021).
19. Starr, T. N. *et al*. Prospective mapping of viral mutations that escape antibodies used to treat COVID-19. *Science* **371**, 850-854, (2021).
20. Liu, L. *et al*. Potent neutralizing antibodies against multiple epitopes on SARS-CoV-2 spike. *Nature* **584**, 450-456, (2020).
21. Wang, P. *et al*. Antibody resistance of SARS-CoV-2 variants B.1.351 and B.1.1.7. *Nature* **593**, 130-135, https://doi.org/10.1038/s41586-021-03398-2 (2021).
22. Fafi-Kremer, S. *et al*. Serologic responses to SARS-CoV-2 infection among hospital staff with mild disease in eastern France. *EBioMedicine* **59**, https://doi.org/10.1016/j.ebiom.2020.102915 (2020).
23. Gallais, F. *et al*. Anti-SARS-CoV-2 Antibodies Persist for up to 13 Months and Reduce Risk of Reinfection. *medRxiv*, 2021.2005.2007.21256823, https://doi.org/10.1101/2021.05.07.21256823 (2021).
24. Krammer, F. *et al*. Antibody Responses in Seropositive Persons after a Single Dose of SARS-CoV-2 mRNA Vaccine. *New England Journal of Medicine* **384**, 1372-1374, (2021).
25. Khoury, D. S. *et al*. Neutralizing antibody levels are highly predictive of immune protection from symptomatic SARS-CoV-2 infection. *Nature Medicine*, https://doi.org/10.1038/s41591-021-01377-8 (2021).
26. Bernal, J. L. *et al*. Effectiveness of COVID-19 vaccines against the B.1.617.2 variant. *medRxiv*, 2021.2005.2022.21257658, https://doi.org/10.1101/2021.05.22.21257658 (2021).

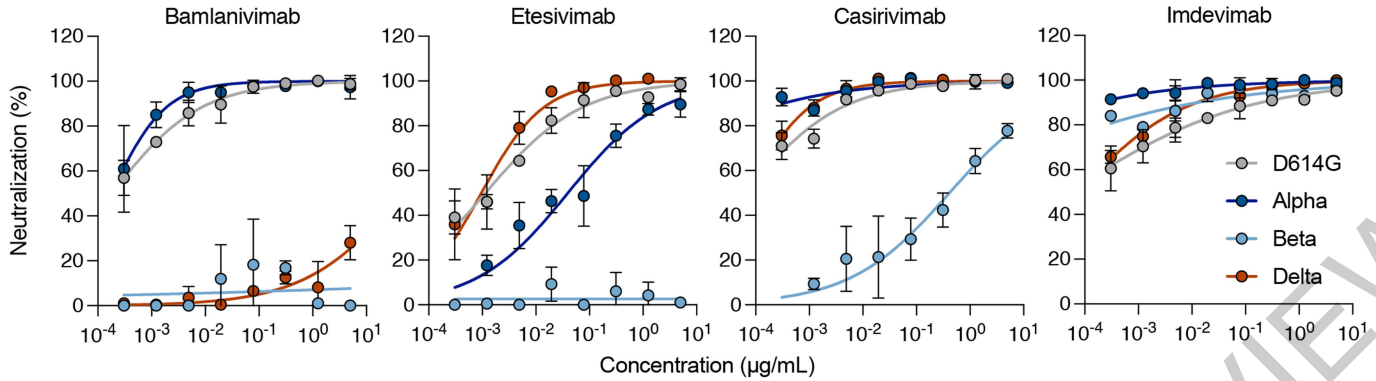

Fig. 1 | Neutralization of SARS-CoV-2 variants D614G, Alpha, Beta and Delta by therapeutic mAbs. Neutralization curves of mAbs. Dose response analysis of the neutralization by four therapeutic mAbs (Bamlanivimab, Etesivimab, Casirivimab and Imdevimab) on D614G strain and variants Alpha, Beta and Delta. Data are mean ± SD of four independent experiments.

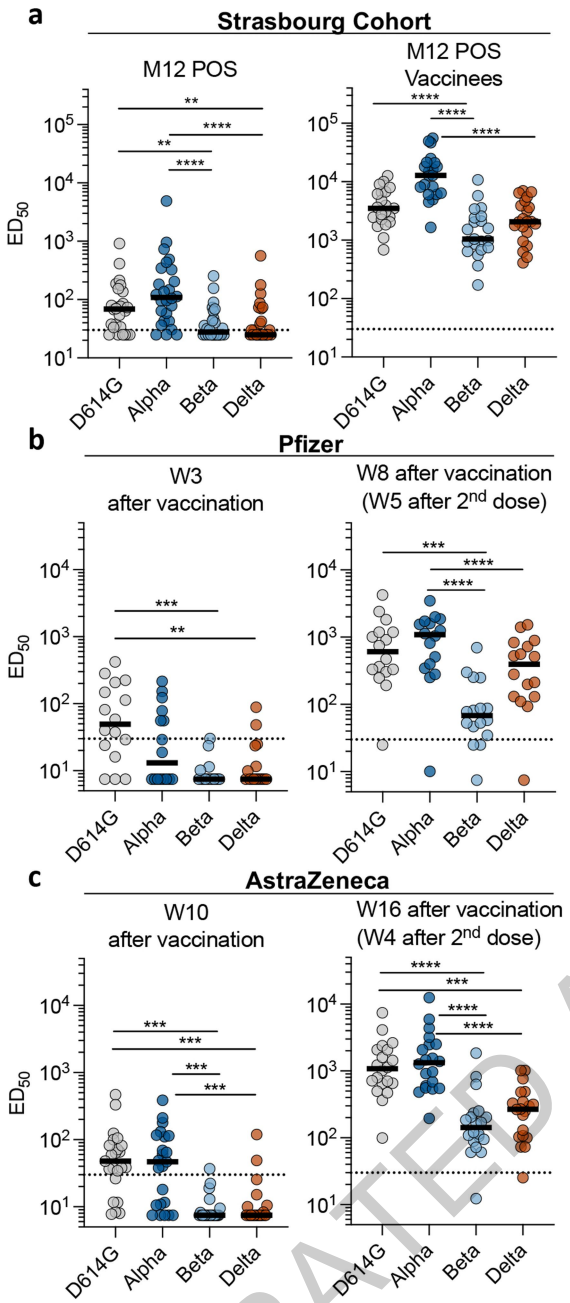

Fig. 2 | Sensitivity of SARS-CoV-2 variants D614G, Alpha, Beta and Delta to sera from convalescent individuals and vaccine recipients. Neutralization titers of the sera against the indicated viral isolates are expressed as ED50. **a**. Neutralizing activity of sera from the Strasbourg cohort of convalescent (n=26, left panel) and convalescent and vaccinated individuals (n=21, right panel) were sampled at Month 12 (M12) post onset of symptoms (POS). **b**. Neutralizing activity of sera from Pfizer vaccinated recipients sampled at W3 (n=16) (left panel) and W8 post-vaccination (W5 after second dose) (n=16) (right panel). **c**. Neutralizing activity of sera from AstraZeneca vaccinated recipients sampled at W10 (n=23) (left panel) and W16 post-vaccination (W4 post second dose) (n=20) (right panel). The dotted line indicates the limit of detection (ED50=30). Data are mean from two independent experiments. Two-sided Friedman test with Dunn's multiple comparison was performed between each viral strain. *$P < 0.05$, **$P < 0.01$, ***$P < 0.001$, ****$P < 0.0001$. M12 POS: D614G versus Beta, $P = 0.0052$; D614G versus Delta, $P = 0.0052$; Alpha versus Beta, $P < 0.0001$; Alpha versus Delta, $P < 0.0001$. M12 POS Vaccinees: D614G versus Beta, $P < 0.0001$; Alpha versus Beta, $P < 0.0001$; Alpha versus Delta, $P < 0.0001$. Pfizer (W3): D614G versus Beta, $P = 0.0001$; D614G versus Delta, $P = 0.0013$. Pfizer (W8): D614G versus Beta, $P = 0.0002$; Alpha versus Beta, $P < 0.0001$; Alpha versus Delta, $P = 0.0098$. AstraZeneca (W10): D614G versus Beta, $P<0.0001$; D614G versus Delta, $P<0.0001$; Alpha versus Beta, $P = 0.0006$; Alpha versus Delta, $P = 0.0056$. AstraZeneca (W16): D614G versus Beta, $P < 0.0001$; D614G versus Delta, $P =0.0375$, Alpha versus Beta, $P < 0.0001$; Alpha versus Delta, $P =0.0375$.

Methods

No statistical methods were used to predetermine sample size. The experiments were not randomized and the investigators were not blinded to allocation during experiments and outcome assessment. Our research complies with all relevant ethical regulation.

Orléans Cohort of convalescent and vaccinated individuals

Since August 27, 2020, a prospective, monocentric, longitudinal, interventional cohort clinical study enrolling 170 SARS-CoV-2-infected individuals with different disease severities, and 59 non-infected healthy controls is on-going, aiming to describe the persistence of specific and neutralizing antibodies over a 24-months period. This study was approved by the ILE DE FRANCE IV ethical committee. At enrolment, written informed consent was collected and participants completed a questionnaire which covered sociodemographic characteristics, virological findings (SARS-CoV-2 RT-PCR results, including date of testing), clinical data (date of symptom onset, type of symptoms, hospitalization), and data related to anti-SARS-CoV-2 vaccination if ever (brand product, date of first and second doses). Serological status of participants was assessed every 3 months. Those who underwent anti-SARS-CoV-2 vaccination had regular blood sampling after first dose of vaccine (ClinicalTrials.gov Identifier: NCT04750720). The primary outcome was the presence of antibodies to SARS-CoV-2 Spike protein as measured with the S-Flow assay. The secondary outcome was the presence of neutralizing antibodies as measured with the S-Fuse assay. For the present study, we selected 56 convalescent and 59 vaccinated participants (16 with Pfizer and 43 with AstraZeneca). Study participants did not receive any compensation.

Strasbourg Cohort of convalescent individuals

Since April 2020, a prospective, interventional, monocentric, longitudinal, cohort clinical study enrolling 308 RT-PCR-diagnosed SARS-CoV-2 infected hospital staff from the Strasbourg University Hospitals is on-going (ClinicalTrials.gov Identifier: NCT04441684). At enrolment (from April 17, 2020), written informed consent was collected and participants completed a questionnaire which covered sociodemographic characteristics, virological findings (SARS-CoV-2 RT-PCR results including date of testing) and clinical data (date of symptom onset, type of symptoms, hospitalization). This study was approved by Institutional Review Board of Strasbourg University Hospital. The serological status of the participants has been described at Months 3 (M3) and Months 6 (M6) POS[22,23]. Laboratory identification of SARS-CoV-2 was performed at least 10 days before inclusion by RT-PCR testing on nasopharyngeal swab specimens according to current guidelines (Institut Pasteur, Paris, France; WHO technical guidance). The assay targets two regions of the viral RNA-dependent RNA polymerase (RdRp) gene with a threshold of detection of 10 copies per reaction. The primary outcome was the presence of antibodies to SARS-CoV-2 Spike protein as measured with the S-Flow assay. The secondary outcome was the presence of neutralizing antibodies as measured with the S-Fuse assay. For the present study, we randomly selected 47 patients collected at M12 (26 unvaccinated and 21 vaccinated). Study participants did not receive any compensation.

Phylogenetic analysis

All SARS-CoV-2 sequences available on the GISAID EpiCov™ database as of May 21, 2021 were retrieved. A subset of complete and high coverage sequences, as indicated in GISAID, assigned to lineages B.1.617.1, B.1.617.2, B.1.617.3 were randomly subsampled to contain up to 5 sequences per country and epidemiological week in R with packages tidyverse and lubridate. Together with a single B.1.617 sequence this subset was included in the global SARS-CoV-2 phylogeny reconstructed with augur and visualized with auspice as implemented in the Nextstrain pipeline (https://github.com/nextstrain/ncov, version from 21 May 2021)[28]. Within Nextstrain, a random subsampling approach capping a maximum number of sequences per global region was used for the contextual non-B.1.617 sequences. The acknowledgment of contributing and originating laboratories for all sequences used in the analysis is provided in Supplementary Table 1.

3D representation of mutations on B1.617.2 and other variants to the Spike surface

Panels in Fig. 1 were prepared with The PyMOL Molecular Graphics System, Version 2.1 Schrödinger, LLC. The atomic model used (PDB:6XR8) has been previously described[29].

S-Fuse neutralization assay

U2OS-ACE2 GFP1-10 or GFP 11 cells, also termed S-Fuse cells, become GFP+ when they are productively infected by SARS-CoV-2[10,11]. Cells were tested negative for mycoplasma. Cells were mixed (ratio 1:1) and plated at $8x10^3$ per well in a µClear 96-well plate (Greiner Bio-One). The indicated SARS-CoV-2 strains were incubated with serially diluted mAb or sera for 15 minutes at room temperature and added to S-Fuse cells. The sera were heat-inactivated 30 min at 56 °C before use. 18 hours later, cells were fixed with 2% PFA, washed and stained with Hoechst (dilution 1:1,000, Invitrogen). Images were acquired with an Opera Phenix high content confocal microscope (PerkinElmer). The GFP area and the number of nuclei were quantified using the Harmony software (PerkinElmer). The percentage of neutralization was calculated using the number of syncytia as value with the following formula: 100 x (1 – (value with serum – value in "non-infected")/(value in "no serum" – value in "non-infected")). Neutralizing activity of each serum was expressed as the half maximal effective dilution (ED50). ED50 values (in µg/ml for mAbs and in dilution values for sera) were calculated with a reconstructed curve using the percentage of the neutralization at the different concentrations.

Clinical history of the patient infected with B.1.617.2

A 54-year-old man was admitted April, 27, 2021 in the Emergency department of the Hôpital Européen Georges Pompidou hospital in Paris, France, for an acute respiratory distress syndrome with fever. He had no medical background and came back from India (West Bengali and few days spent in Delhi) 10 days before (April 17, 2021), where he stayed 15 days for his work. Onset of symptoms (abdominal pain and fever) was approximately April 18, 2021. The nasopharyngeal swab was tested positive for SARS-CoV-2 at his date of admission. Lung tomo-densitometry showed a mild (10-25%) COVID-19 pneumonia without pulmonary embolism. He initially received oxygen therapy 2 L/min, dexamethasone 6mg/day and enoxaparin 0,4 ml twice a day. His respiratory state worsened on day 3 (April 30, 2021). He was transferred in an intensive care unit, where he received high flow oxygen therapy (maximum 12 L/min). His respiratory condition improved, and he was transferred back in a conventional unit on day 8 (May 5, 2021). He was discharged from hospital on day 15 (May 10, 2021).

Virus strains

The reference D614G strain (hCoV-19/France/GE1973/2020) was supplied by the National Reference Centre for Respiratory Viruses hosted by Institut Pasteur (Paris, France) and headed by Pr. S. van der Werf. This viral strain was supplied through the European Virus Archive goes Global (Evag) platform, a project that has received funding from the European Union's Horizon 2020 research and innovation program under grant agreement n° 653316. The variant strains were isolated from nasal swabs using Vero E6 cells and amplified by one or two passages. B.1.1.7 originated from a patient in Tours (France) returning from United Kingdom. B.1.351 (hCoV-19/France/IDF-IPP00078/2021) originated from a patient in Creteil (France). B.1.617.2 was isolated from a nasopharyngeal swab of a hospitalized patient returning from India. The swab was provided and sequenced by the laboratory of Virology of Hopital Européen Georges Pompidou (Assistance Publique – Hopitaux

de Paris). Both patients provided informed consent for the use of the biological materials. Titration of viral stocks was performed on Vero E6, with a limiting dilution technique allowing a calculation of TCID50, or on S-Fuse cells. Viruses were sequenced directly on nasal swabs, and after one or two passages on Vero cells. Sequences were deposited on GISAID immediately after their generation, with the following IDs: D614G: EPI_ISL_414631; B.1.1.7: EPI_ISL_735391; B.1.1.351: EPI_ISL_964916; B.1.617.2: ID: EPI_ISL_2029113.

Flow Cytometry

Vero cells were infected with the indicated viral strains at a multiplicity of infection (MOI) of 0.1. Two days after, cells were detached using PBS-EDTA and transferred into U-bottom 96-well plates (50,000 cell/well). Cells were fixed in 4% PFA for 15-30 min at RT. Cells were then incubated for 15-30 min at RT with the indicated mAbs (1 µg/mL) in PBS, 1% BSA, 0.05% sodium azide, and 0.05% Saponin. Cells were washed with PBS and stained using anti-IgG AF647 (1:600 dilution) (ThermoFisher). Stainings were also performed on control uninfected cells. Data were acquired on an Attune Nxt instrument using Attune Nxt Software v3.2.1 (Life Technologies) and analysed with FlowJo 10.7.1 (Becton Dickinson).

Antibodies

The four therapeutic antibodies were kindly provided by CHR Orleans. Human anti-SARS-CoV2 mAbs were cloned from S-specific blood memory B cells of COVID-19 convalescents (Planchais et al, manuscript in preparation). Recombinant human IgG1 mAbs were produced by co-transfection of Freestyle 293-F suspension cells (Thermo Fisher Scientific) as previously described[30], purified by affinity chromatography using protein G sepharose 4 fast flow beads (GE Healthcare) and validated using ELISA against the trimeric S, RBD, S2 and NTD proteins (Planchais et al, in preparation).

Statistical analysis

Flow cytometry data were analyzed with FlowJo v10 software (TriStar). Calculations were performed using Excel 365 (Microsoft). Figures were drawn on Prism 9 (GraphPad Software). Statistical analysis was conducted using GraphPad Prism 9. Statistical significance between different groups was calculated using the tests indicated in each figure legend.

Reporting summary

Further information on research design is available in the Nature Research Reporting Summary linked to this paper.

Data availability

All data supporting the findings of this study are available within the article or from the corresponding authors upon request. Source data are provided with this paper. Viral sequences are available upon request and were deposited at GISAID (https://www.gisaid.org/) under the following numbers: hCoV-19/France/GE1973/2020 (D614G): EPI_ISL_414631; Alpha (B.1.1.7): EPI_ISL_735391; Beta (B.1.351): EPI_ISL_964916 and Delta (B.1.617.2): EPI_ISL_2029113. Source data are provided with this paper.

27. Tzou, P. L. *et al*. Coronavirus Antiviral Research Database (CoV-RDB): An Online Database Designed to Facilitate Comparisons between Candidate Anti-Coronavirus Compounds. *Viruses* **12**, 1006 (2020).
28. Hadfield, J. *et al*. Nextstrain: real-time tracking of pathogen evolution. *Bioinformatics* **34**, 4121-4123, (2018).
29. Cai, Y. *et al*. Distinct conformational states of SARS-CoV-2 spike protein. *Science* **369**, 1586-1592(2020).
30. Lorin, V. & Mouquet, H. Efficient generation of human IgA monoclonal antibodies. *J Immunol Methods* **422**, 102-110, (2015).

Acknowledgements We thank Nicoletta Casartelli for critical reading of the manuscript and Pablo Guardado Calvo for discussion. We thank patients who participated to this study, members of the Virus and Immunity Unit for discussions and help, Nathalie Aulner and the UtechS Photonic BioImaging (UPBI) core facility (Institut Pasteur), a member of the France BioImaging network, for image acquisition and analysis. The Opera system was co-funded by Institut Pasteur and the Région ile de France (DIM1Health))We thank the DRCI, CIC, Médecine du travail and Pôle de Biologie teams (CHU de Strasbourg) for the management of the Strasbourg cohort and serology testing. We thank the members of the Virus and Immunity Unit for discussion and help, the UTechS Photonic BioImaging (PBI) core facility (Institut Pasteur), a member of the France BioImaging network, for image acquisition and analysis (the Opera system was co-funded by Institut Pasteur and the Région ile de France (DIM1Health)). Work in OS lab is funded by Institut Pasteur, Urgence COVID-19 Fundraising Campaign of Institut Pasteur, Fondation pour la Recherche Médicale (FRM), ANRS, the Vaccine Research Institute (ANR-10-LABX-77), Labex IBEID (ANR-10-LABX-62-IBEID), ANR/FRM Flash Covid PROTEO-SARS-CoV-2 and IDISCOVR. Work in UPBI is funded by grant ANR-10-INSB-04-01 and Région Ile-de-France program DIM1-Health. DP is supported by the Vaccine Research Institute. LG is supported by the French Ministry of Higher Education, Research and Innovation. HM lab is funded by the Institut Pasteur, the Milieu Intérieur Program (ANR-10-LABX-69-01), the INSERM, REACTing, EU (RECOVER) and Fondation de France (#00106077) grants. SFK lab is funded by Strasbourg University Hospitals (SeroCoV-HUS; PRI 7782), Programme Hospitalier de Recherche Clinique (PHRC N 2017– HUS N° 6997), the Agence Nationale de la Recherche (ANR-18-CE17-0028), Laboratoire d'Excellence TRANSPLANTEX (ANR-11-LABX-0070_TRANSPLANTEX), Institut National de la Santé et de la Recherche Médicale (UMR_S 1109). ESL lab is funded by Institut Pasteur and the French Government's Investissement d'Avenir programme, Laboratoire d'Excellence "Integrative Biology of Emerging Infectious Diseases" (grant n°ANR-10-LABX-62-IBEID). The funders of this study had no role in study design, data collection, analysis and interpretation, or writing of the article.

Author contributions Experimental strategy design, experiments: DP, DV, AB, IS, FGB, MMR, FP, TB, ESL, FR. Vital materials DV, CP, NR, JP, MP, FG, PG, AV, JLG, LC, NKC, DE, LB, AS, HP, LH, SFK, TP, HM. Manuscript writing: DP, TB, ESL, FR, OS. Manuscript editing: DV, MMR, HP, LH, SFK, TP, HM.

Competing interests C.P., H.M., O.S, T.B., F.R. have a pending patent application for the anti-RBD mAbs described in the present study (PCT/FR2021/070522).

Additional information

Supplementary information The online version contains supplementary material available at https://doi.org/10.1038/s41586-021-03777-9.

Correspondence and requests for materials should be addressed to T.B. or O.S.

Peer review information *Nature* thanks the anonymous reviewers for their contribution to the peer review of this work.

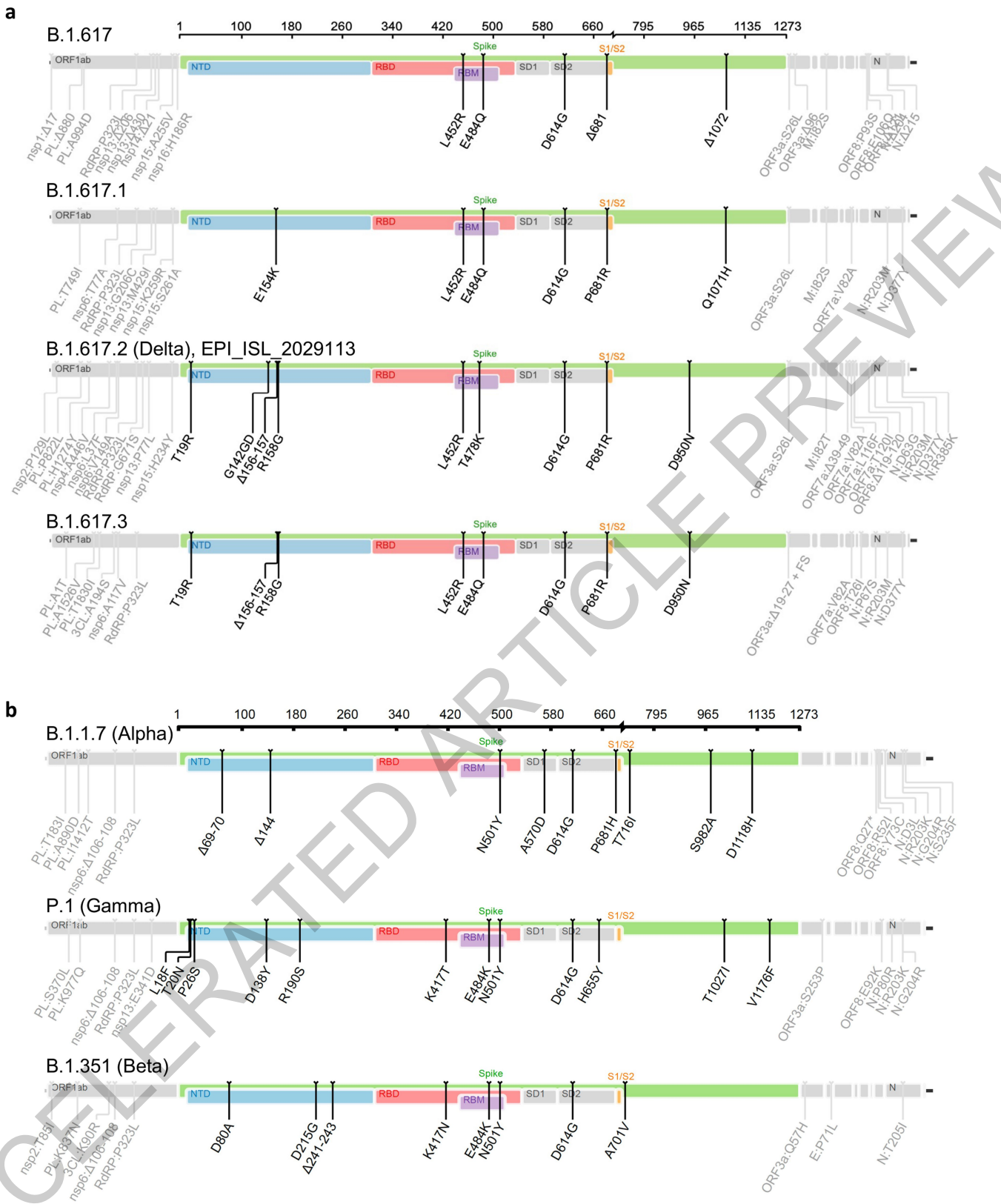

Extended Data Fig. 1 | Schematic overview of the B.1.617 sublineage and variants of concern. Schematic overview of B.1.617 sublineage **(a)** and variants of concern B.1.1.7 (Alpha), P1 (Gamma) and B.1.351 (Beta) **(b)**. Consensus sequences with a focus on the Spike were built with the Sierra tool[27]. Amino acid modifications in comparison to the ancestral Wuhan-Hu-1 sequence (NC_045512) are indicated.

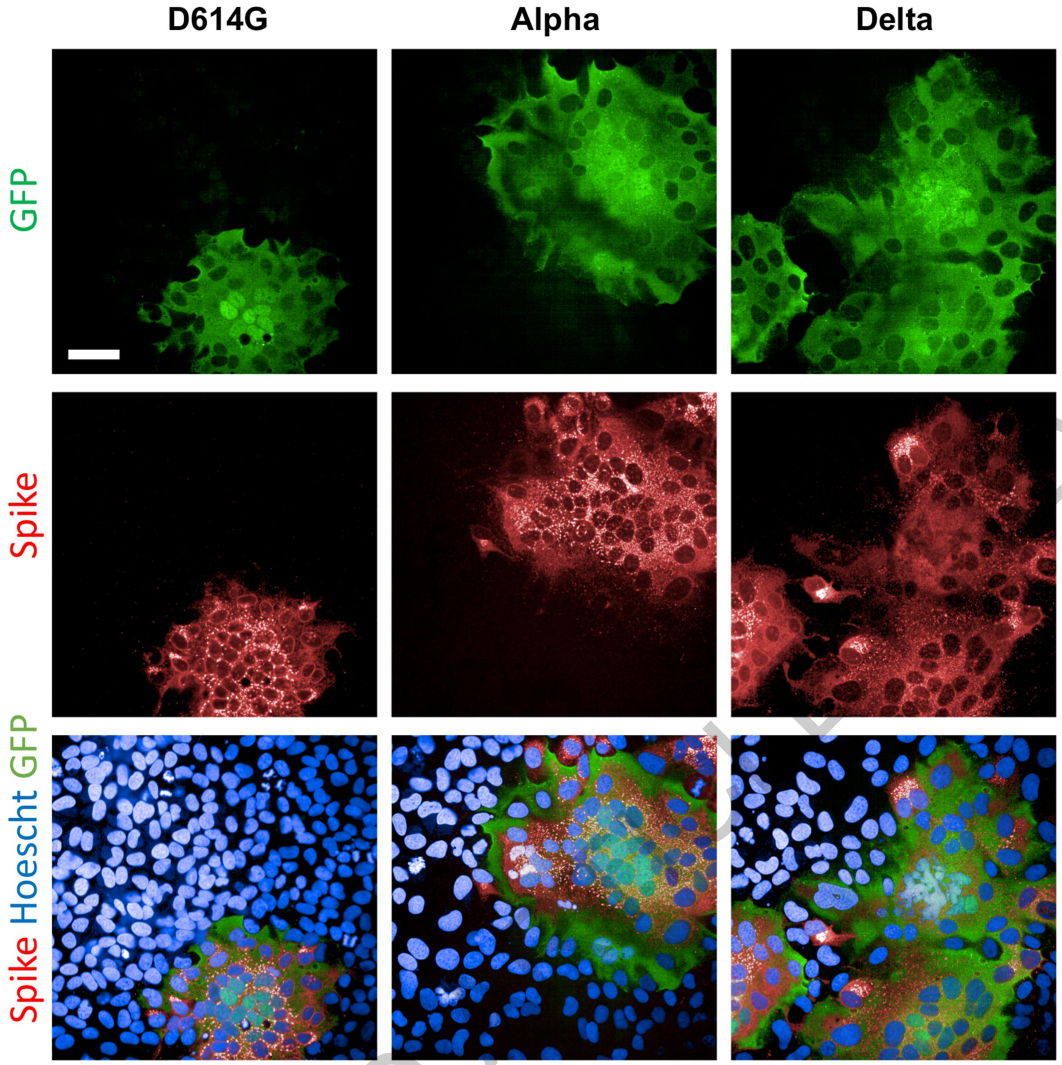

Extended Data Fig. 2 | SARS-CoV-2 variants induce syncytia in S-Fuse cells. S-Fuse cells were exposed to the indicated SARS-CoV-2 strain (MOI 10^{-3}). The cells become GFP+ when they fuse together. After 20 h, infected cells were stained with anti-Spike antibodies and Hoechst to visualize nuclei. Syncytia (green), Spike (red) and nuclei (blue) are shown. Representative images from three independent experiments are shown. Scale bar: 50 µm.

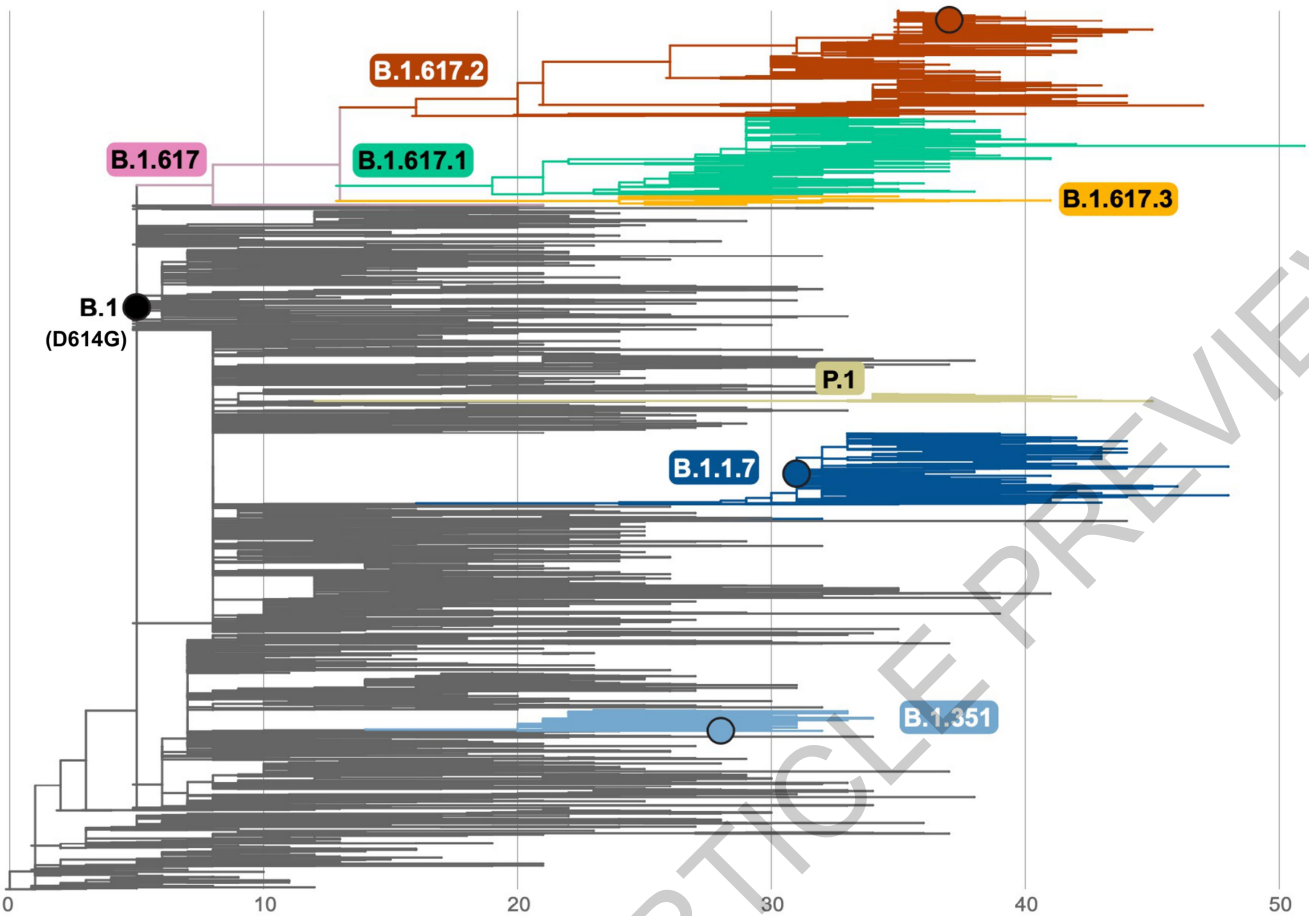

Extended Data Fig. 3 | Global phylogeny of SARS-CoV-2 highlighting the B.1.617 lineage. The maximum likelihood tree was inferred using IQ-Tree, as implemented in the Nextstrain pipeline on a subsampled dataset of 3794 complete genomes. Branch lengths are scaled according to the number of nucleotide substitutions from the root of the tree. The branches corresponding to key lineages are colored: B.1.1.7, dark blue; B.1.351, light blue; P.1, beige; B.1.617, pink; B.1.617.1, green; B.1.617.2, red; B.1.617.3, orange. A black circle indicates the position of the viruses studied here.

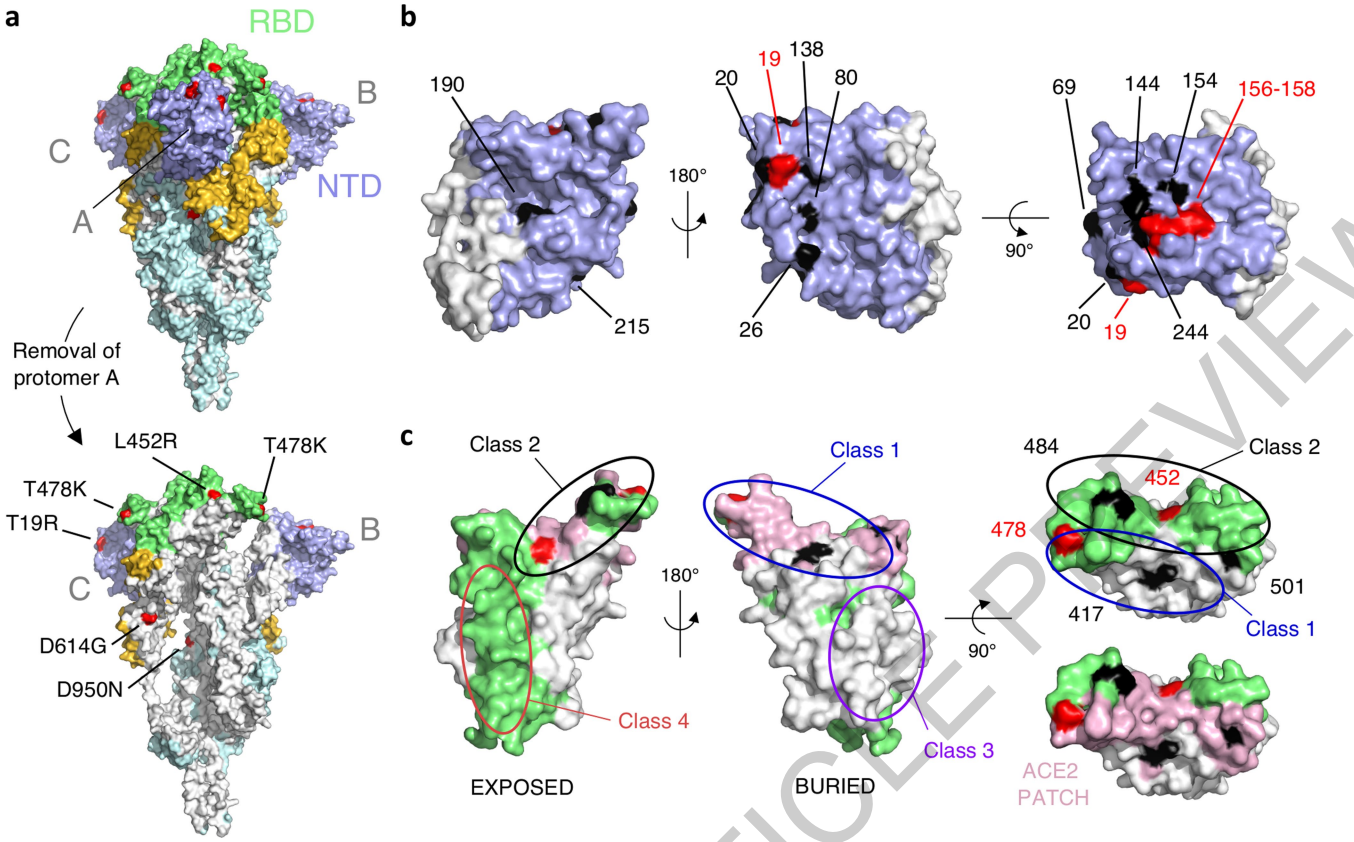

Extended Data Fig. 4 | Mapping mutations of variant Delta and other variants of concern to the Spike surface. a. The Spike protein trimer (PDB:6XR8, corresponding to a closed spike trimer with all three RBDs in the "down" conformation) is shown with its surface colored according to domains: NTD in dark blue, RBD in green, the remainder of S1 in yellow and S2 in light blue. Interfaces between protomers were left white to help visualize the protomers' boundaries. The three polypeptide chains in the trimer were arbitrarily defined as A, B and C. Surface patches corresponding to residues mutated in the variant Delta are colored in red. The bottom panel has the front protomer (chain A) removed to show the trimer interface (buried regions in the trimer are in white). The mutations in Delta are labelled in the bottom panel. **b**. NTD shown in three orthogonal views. The left panel corresponds roughly to the orientation seen in chain B in a, and the middle panel shows a view from the back. The right panel shows a view from the top of the trimer. Mutations found in the main variants of concern are indicated. The mutations found in variant Delta are in red. **c**. RBD shown in three orthogonal views, colored according to solvent exposure in the context of the closed spike: green and white indicate exposed and buried surfaces, as in a. The ACE2-binding surface is colored in pink. The left panel shows a view from the top of the trimer, and the middle panel a view from below. The right panels show a view down the ACE2 binding surface, highlighted in pink in the bottom panel. Mutations found in the main variants of concern are indicated. The mutations found in variant Delta are in red. The ovals indicate the epitope regions of the four main classes of anti-RBD neutralizing antibodies. Note that the mutations on the RBD cluster all around the ACE2 patch. Panels were prepared with The PyMOL Molecular Graphics System, Version 2.1 Schrödinger, LLC.

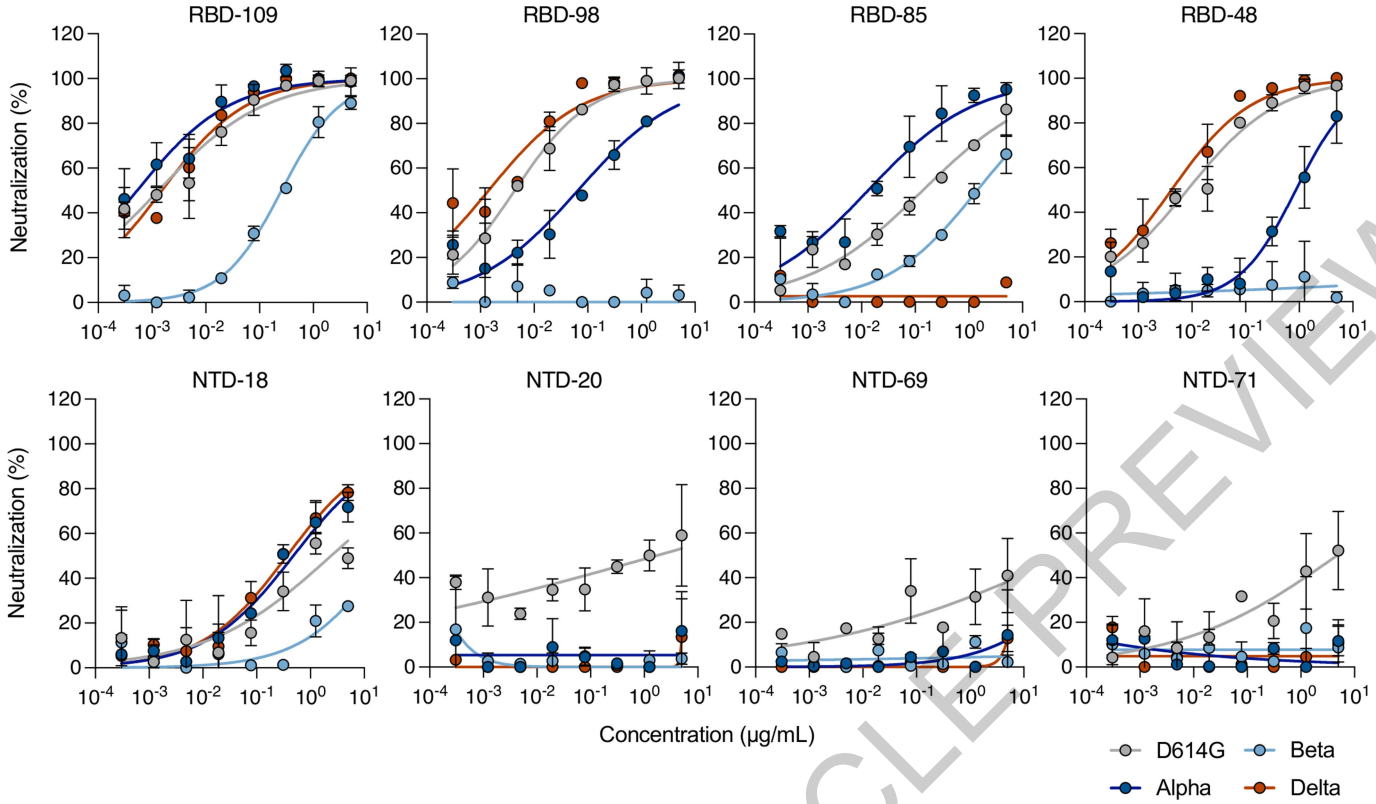

Extended Data Fig. 5 | Neutralization of SARS-CoV-2 variants D614G, Alpha, Beta and Delta by mAbs targeting the RBD and the NTD domains. Neutralization curves of mAbs. Dose response analysis of the neutralization by four anti-RBD and four anti-NTD on D614G strain (grey), and variants Alpha (dark blue), Beta (light blue) and Delta (orange). Data are mean ± SD of three independent experiments.

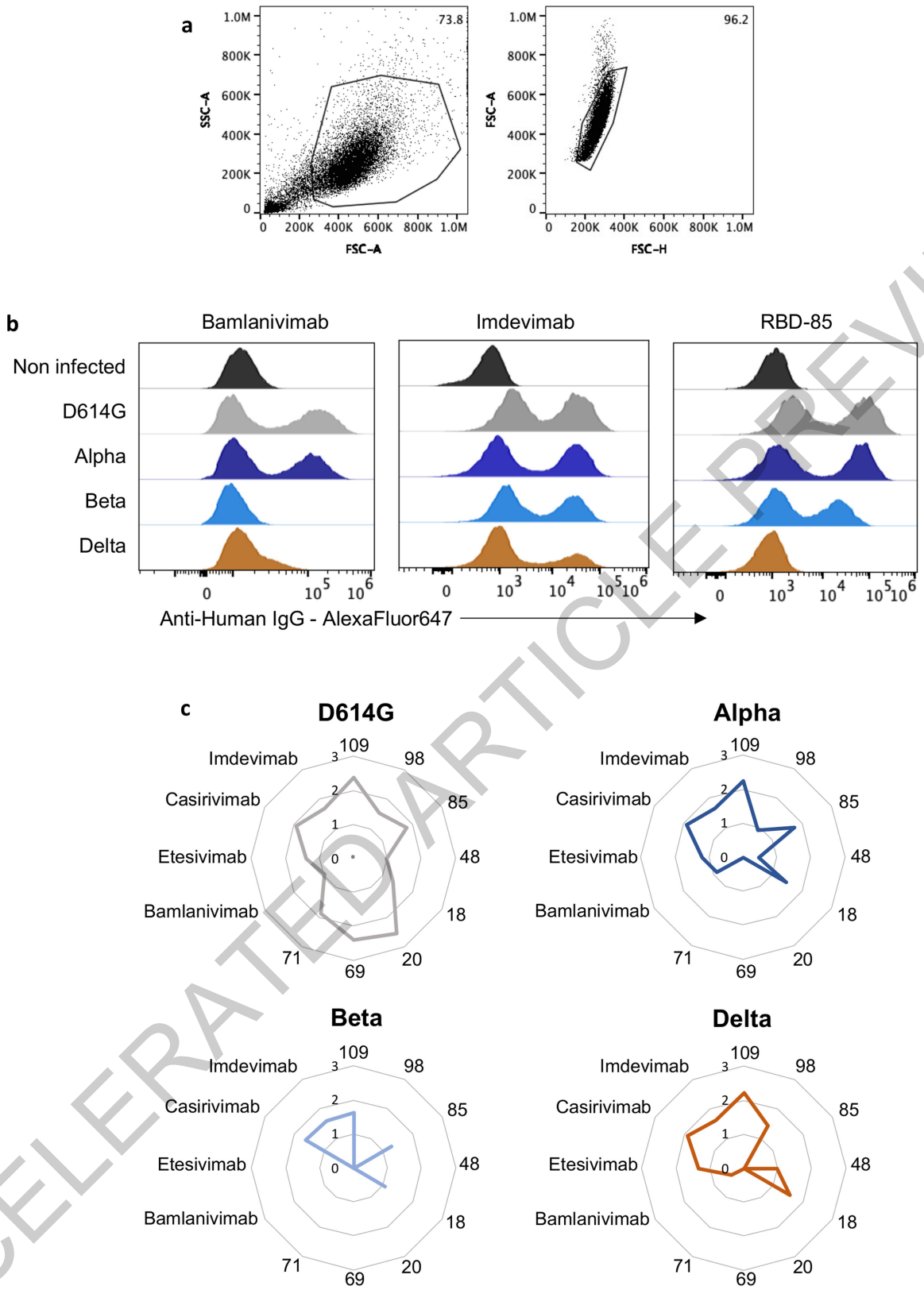

Extended Data Fig. 6 | Binding of anti-SARS-CoV-2 mAbs to Vero cells infected with variants D614G, Alpha, Beta and Delta. Vero cells were infected with the indicated variants at a MOI of 0.1. After 48h, cells were stained with anti-SARS-CoV-2 mAbs (1µg/ml) and analyzed by flow-cytometry. **a**. Gating strategy. **b**. Histograms show the binding of Bamlanivimab, Imdevimab and RBD-85 to Vero cells infected with the indicated variants. **c**. Radar charts represent for each antibody the logarithm of the mean of fluorescent intensity of the staining, relative to the non-infected condition. Data are representative of three independent experiments.

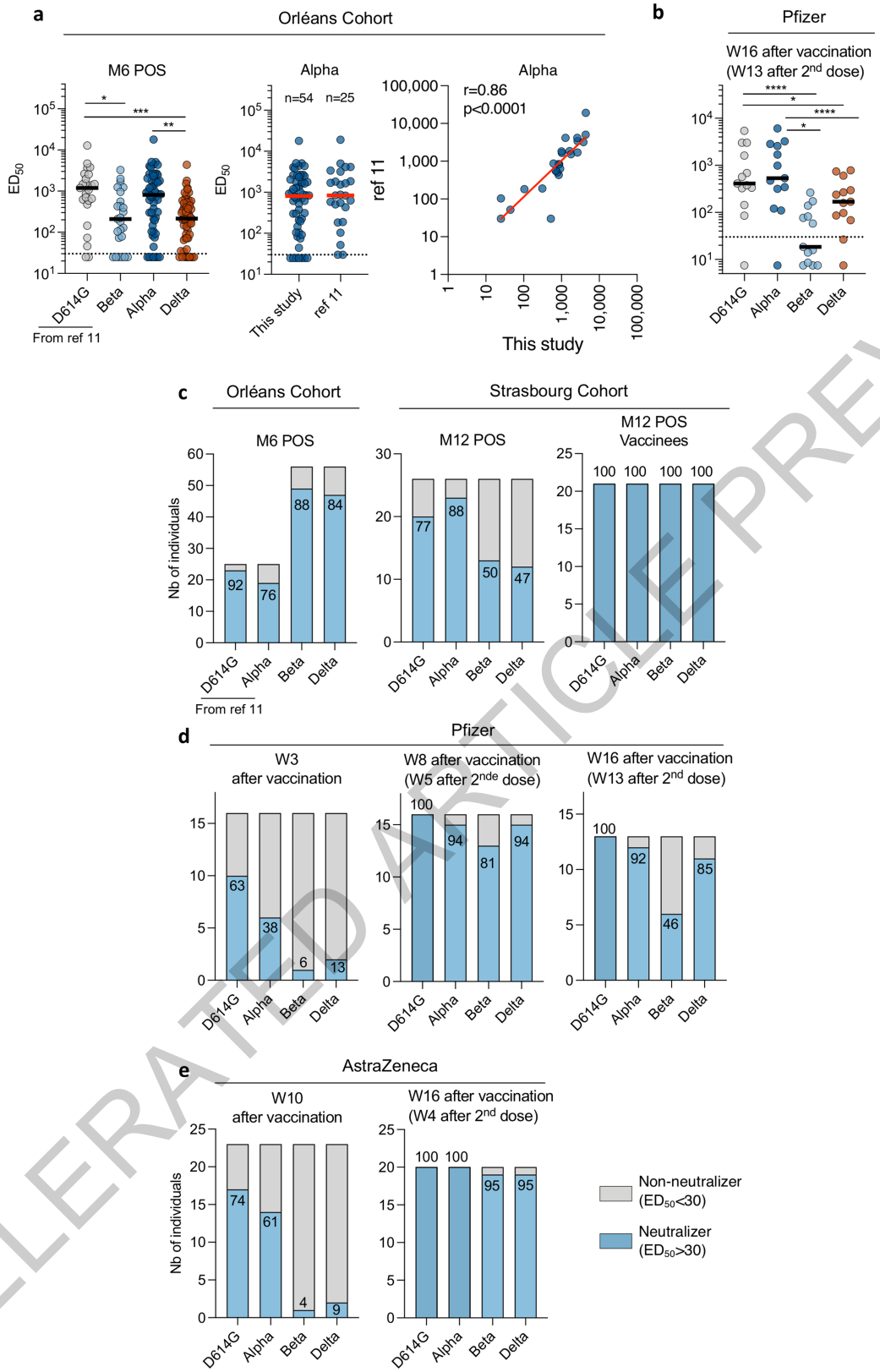

Extended Data Fig. 7 | See next page for caption.

Extended Data Fig. 7 | Sensitivity of SARS-CoV-2 variants D614G, Alpha, Beta and Delta to sera from convalescent individuals and vaccine recipients. a. ED50 of neutralization of convalescent individuals from the Orléans cohort against the four viral variants are depicted. Samples were collected 6 months post onset of symptoms (M6 POS). Sensitivity of variants D614G and Alpha was assessed on 25 individuals previously published in ref. [11]. Fifty six sera (including the 25 previous sera) were tested against variants Beta and Delta. Neutralization data obtained in this study and in ref. [11] were compared (middle panel) and correlated (right panel). Similar results were obtained, allowing to bridge the datasets. Data are mean from two independent experiments. The dotted line indicates the limit of detection (ED50=30). Two-sided Kruskal-Wallis test with Dunn's multiple comparison was performed between each viral strain. *$P < 0.05$, **$P < 0.01$, ***$P < 0.001$, ****$P < 0.0001$. D614G versus Beta, $P = 0.0153$; D614G versus Delta, $P = 0.0008$; Alpha versus Delta, $P = 0.0014$. **b**. ED50 of neutralization of Pfizer-vaccinated individuals sampled at W16 (corresponding to W13 after the second dose). Data are mean from two independent experiments. The dotted line indicates the limit of detection (ED50=30). Two-sided Kruskal-Wallis test with Dunn's multiple comparison was performed between each viral strain. *$P < 0.05$, **$P < 0.01$, ***$P < 0.001$, ****$P < 0.0001$. D614G versus Beta, $P < 0.0001$; D614G versus Delta, $P = 0.0375$; Alpha versus Beta, $P < 0.0001$; Alpha versus Delta, $P = 0.0375$. **c,d,e**. Fraction of neutralizers in the cohorts of convalescent or vaccinated individuals. Individuals with an ED50 of neutralization above 30 were categorized as neutralizers and are indicated in blue. Non-neutralizers are in grey. **c**. Analysis of convalescent individuals from the Orléans cohort collected at M6 (left panel, related to Extended Data Fig. 7a.), from the Strasbourg cohort collected at M12 and unvaccinated (middle panel, related to Fig. 2a) or vaccinated (right panel, related to Fig. 2a). **c**. Sera from Pfizer vaccinated recipients were sampled at W3, W8 (left and middle panels, related to Fig. 2c), and W16 post-vaccination (related to Extended Data Fig. 7b). **e**. Sera from AstraZeneca vaccinated recipients sampled at W10 and W16 post-vaccination (related to Fig. 2c). The numbers indicate the % of neutralizers.

Extended Data Table 1 | Characteristics of the two cohorts of convalescent individuals

a.

Orléans Cohort: M6 POS		**n=56**
Sex		
	Female	29
	Male	27
Age (Median; range)		53 (22;77)
Severity		
	Critical	13
	Severe	15
	Mild-Moderate	16
	Asymptomatic	12
HIV		3
PCR		53
Anti-S (S-Flow)		56
Sampling days POS (median; range)		188 (114;205)

b.

Strasbourg Cohort : M12 POS		**Convalescent n=26**	**Vaccinated Convalescent n=21**
Sex			
	Female	21	18
	Male	5	3
Age (Median; range)		36 (24;60)	44 (23;62)
Severity			
	Critical	0	0
	Severe	0	0
	Mild-Moderate	26	21
	Asymptomatic	0	0
PCR		26	21
Anti-S (Abott)		26	21
Vaccine			
	AstraZeneca	0	9
	Pfizer	0	9
	Moderna	0	3
Sampling days (median; range)			
	POS	330 (144;383)	359 (327;404)
	Post Vaccine	NA	24 (7;81)

Extended Data Table 2 | Characteristics of the cohort of vaccinated recipients

Orléans cohort: Vaccinated recipients		Pfizer (1 or 2 doses) n=16	AstraZeneca (1 dose) n=23	AstraZeneca (2 doses) N=20
Sex				
	Female	5	7	15
	Male	11	5	5
Age (Median; range)		60 (35;75)	38 (28;64)	59.5 (55;73)
Immune deficiency		0	0	0
Previous COVID-19		0	0	0
Anti-N		0	0	0
1st dose		Jan 4 – 8, 2021	Feb 8 – April 22, 2021	Feb 5 – April 7, 2021
2nd dose		Jan 20 – Feb 5, 2021	NA	May 3 – 19, 2021
Sampling days post-vaccination (Median; range)				
	W3	20 (18;25)		
	W8	57 (53;84)		
	W10		70 (41;91)	
	W16	118 (116;124)		109 (56;116)

nature research

Corresponding author(s): Timothée Bruel, Olivier Schwartz

Last updated by author(s): Jun 17, 2021

Reporting Summary

Nature Research wishes to improve the reproducibility of the work that we publish. This form provides structure for consistency and transparency in reporting. For further information on Nature Research policies, see our Editorial Policies and the Editorial Policy Checklist.

Statistics

For all statistical analyses, confirm that the following items are present in the figure legend, table legend, main text, or Methods section.

n/a	Confirmed	
☐	☒	The exact sample size (*n*) for each experimental group/condition, given as a discrete number and unit of measurement
☐	☒	A statement on whether measurements were taken from distinct samples or whether the same sample was measured repeatedly
☐	☒	The statistical test(s) used AND whether they are one- or two-sided *Only common tests should be described solely by name; describe more complex techniques in the Methods section.*
☐	☒	A description of all covariates tested
☐	☒	A description of any assumptions or corrections, such as tests of normality and adjustment for multiple comparisons
☐	☒	A full description of the statistical parameters including central tendency (e.g. means) or other basic estimates (e.g. regression coefficient) AND variation (e.g. standard deviation) or associated estimates of uncertainty (e.g. confidence intervals)
☐	☒	For null hypothesis testing, the test statistic (e.g. *F*, *t*, *r*) with confidence intervals, effect sizes, degrees of freedom and *P* value noted *Give P values as exact values whenever suitable.*
☒	☐	For Bayesian analysis, information on the choice of priors and Markov chain Monte Carlo settings
☒	☐	For hierarchical and complex designs, identification of the appropriate level for tests and full reporting of outcomes
☒	☐	Estimates of effect sizes (e.g. Cohen's *d*, Pearson's *r*), indicating how they were calculated

Our web collection on statistics for biologists contains articles on many of the points above.

Software and code

Policy information about availability of computer code

Data collection	Harmony Software v4.9 (Perkin-Elmer), Attune Nxt Software v3.2.1 (ThermoFischer), Flowjo Software v10.7.1, R v4.1.0, tidyverse v1.3.1, Lubridate v1.7.10
Data analysis	Excel 365 v16.46 (Microsoft), Prism v9.0.2 (GraphPad Software)

For manuscripts utilizing custom algorithms or software that are central to the research but not yet described in published literature, software must be made available to editors and reviewers. We strongly encourage code deposition in a community repository (e.g. GitHub). See the Nature Research guidelines for submitting code & software for further information.

Data

Policy information about availability of data

All manuscripts must include a data availability statement. This statement should provide the following information, where applicable:

- Accession codes, unique identifiers, or web links for publicly available datasets
- A list of figures that have associated raw data
- A description of any restrictions on data availability

All data are provided as supplementary tables

Field-specific reporting

Please select the one below that is the best fit for your research. If you are not sure, read the appropriate sections before making your selection.

☒ Life sciences ☐ Behavioural & social sciences ☐ Ecological, evolutionary & environmental sciences

For a reference copy of the document with all sections, see nature.com/documents/nr-reporting-summary-flat.pdf

Life sciences study design

All studies must disclose on these points even when the disclosure is negative.

Sample size	162 sera from convalescent, vaccinated and vaccinated convalescent individuals were analyzed in the study. Given the explanatory nature of the study aiming at describing a phenomenon whose frequency has not yet been established we did not use statistical methods to predetermine sample size. Thus, we included between 20 and 50 patients per group to allow statistical analysis
Data exclusions	None.
Replication	All experiments were performed and verified in multiple replicates as indicated in their methods/figure legends.
Randomization	The experiments were not randomized as this is not relevant for an observationnal study.
Blinding	The investigators were not blinded to allocation as this is not relevant for an observationnal study. However, the clinical sampling and biological measurement were performed by different teams. Only the final assembly of the data revealed the global view of the results.

Reporting for specific materials, systems and methods

We require information from authors about some types of materials, experimental systems and methods used in many studies. Here, indicate whether each material, system or method listed is relevant to your study. If you are not sure if a list item applies to your research, read the appropriate section before selecting a response.

Materials & experimental systems

n/a	Involved in the study
☐	☒ Antibodies
☐	☒ Eukaryotic cell lines
☒	☐ Palaeontology and archaeology
☒	☐ Animals and other organisms
☐	☒ Human research participants
☐	☒ Clinical data
☒	☐ Dual use research of concern

Methods

n/a	Involved in the study
☒	☐ ChIP-seq
☐	☒ Flow cytometry
☒	☐ MRI-based neuroimaging

Antibodies

Antibodies used	The anti-S RBD-48, RBD-85, RBD-98, RBD-109, NTD-18, NTD-20, NTD-69 and NTD-71 are human anti-S monoclonal antibodies isolated and produced by Hugo Mouquet (Institut Pasteur). Bamlanivimab, Etesivimab, Casirivimab and Imdevimab are kind gifts of Thierry Prazuck and Laurent Hocqueloux. The Goat anti-Human IgG (H+L) Cross-Adsorbed Secondary Antibody, Alexa Fluor 647 (A21445) was obtained from thermoFisher Scientific.
Validation	The human anti-S RBD-48, RBD-85, RBD-98, RBD-109, NTD-18, NTD-20, NTD-69 and NTD-71 were validated using ELISAs (against the trimeric S, RBD, S2 and NTD proteins) by the team of H.Mouquet. Bamlanivimab, Etesivimab, Casirivimab and Imdevimab were validated by measuring their binding and neutralizing activity against SARS-CoV-2. Validation of the goat anti-human IgG is available from the ThermoFisher website.

Eukaryotic cell lines

Policy information about cell lines

Cell line source(s)	Vero E6 (ATCC® CRL-1586™), Freestyle 293-F (ThermoFisher) and U2OS cells (ATCC® HTB-96™), all obtained from the ATCC.
Authentication	Cell lines were not authenticated.
Mycoplasma contamination	All cells are negative for mycoplasma contamination. Tests are performed on a bi-monthly basis

Commonly misidentified lines (See ICLAC register)	None

Human research participants

Policy information about studies involving human research participants

Population characteristics	Orleans' Cohort of convalescent and/or vaccinated individuals: since April 2020, a prospective, monocentric, longitudinal, cohort clinical study enrolling 170 SARS-CoV-2-infected individuals and 59 non-infected healthy controls is on-going, aiming to describe the persistence of specific and neutralizing antibodies over a 24-months period. Relevant co-variates are available in extended table 1a and 2. Strasbourg Cohort of convalescent individuals: Since April 2020, a prospective, interventional, monocentric, longitudinal, cohort clinical study enrolling 308 RT-PCR-diagnosed SARS-CoV-2 infected hospital staff from the Strasbourg University Hospitals is on-going. Given the exploratory design of the two studies, the characteristics of participants were not pre-established when entering the cohorts. Relevant co-variates are available in extended table 1b.
Recruitment	Orléans cohort : Individuals admitted to the hospital for COVID-19 or with known COVID-19 consulting for a chronic disease were invited to participate. Strasbourg Cohort : Hospital staff with PCR-confirmed COVID-19 were invited to participate. Individuals were included without any selection other than those imposed by the entry criteria (known COVID-19 or vaccination). Under these conditions, no particular bias is envisaged.
Ethics oversight	Orléans was approved by national external committee (CPP Ile de France IV, IRB No. 00003835). Strasbourg cohort was approved by the institutional review board of Strasbourg University Hospitals. At enrolment a written informed consent was collected for all participants.

Note that full information on the approval of the study protocol must also be provided in the manuscript.

Clinical data

Policy information about clinical studies

All manuscripts should comply with the ICMJE guidelines for publication of clinical research and a completed CONSORT checklist must be included with all submissions.

Clinical trial registration	NCT04750720 and NCT04441684
Study protocol	All protocols can be accessed on clinicaltrial.gov
Data collection	Orléans and strasbourg cohorts started on April 2020 in Strasbourg Hospital (Hopitaux universitaires de Strasbourg) and Orléans Hospital (Centre hospitalier Régional Orléans) respectively, and are on-going.
Outcomes	The primary outcome of both studies was the presence of antibodies to SARS-CoV-2 Spike protein as measured with the S-Flow assay. The secondary outcome was the presence of neutralizing antibodies as measured with the S-Fuse assay.

Flow Cytometry

Plots

Confirm that:

☒ The axis labels state the marker and fluorochrome used (e.g. CD4-FITC).

☒ The axis scales are clearly visible. Include numbers along axes only for bottom left plot of group (a 'group' is an analysis of identical markers).

☒ All plots are contour plots with outliers or pseudocolor plots.

☒ A numerical value for number of cells or percentage (with statistics) is provided.

Methodology

Sample preparation	SARS-CoV-2 infected Vero cells were stained as indicated in the method section. All samples were acquired within 24h.
Instrument	Attune NxT Acoustic Focusing Cytometer, blue/red/violet/yellow (catalog number : 15360667)
Software	AttuneNxT Software v3.2.1
Cell population abundance	At least 10,000 cells were acquired for each condition.
Gating strategy	All gates were set on uninfected Vero cells.

☒ Tick this box to confirm that a figure exemplifying the gating strategy is provided in the Supplementary Information.